

CARBON-ENHANCED METAL-POOR STARS IN SDSS/SEGUE. II. COMPARISON OF CEMP STAR FREQUENCIES WITH BINARY POPULATION SYNTHESIS MODELS

YOUNG SUN LEE, TAKUMA SUDA, TIMOTHY C. BEERS, AND SARA LUCATELLO

¹Department of Astronomy, New Mexico State University, Las Cruces, NM, 88003, USA; yslee@nmsu.edu

²National Astronomical Observatory of Japan, Osawa 2-21-1, Mitaka, Tokyo 181-8588, Japan

³National Optical Astronomy Observatory, Tucson, AZ 85719, USA

⁴Joint Institute for Nuclear Astrophysics (JINA), Michigan State University, East Lansing, MI 48824, USA

⁵INAF-Osservatorio Astronomico di Padova, vicolo dell'Osservatorio 5, I-35122 Padova, Italy

Submitted on October 10, 2013

ABSTRACT

We present a comparison of the frequencies of carbon-enhanced metal-poor (CEMP) giant and main-sequence turnoff stars, selected from the Sloan Digital Sky Survey (SDSS) and the Sloan Extension for Galactic Understanding and Exploration (SEGUE), with predictions from asymptotic giant-branch (AGB) mass-transfer models. We consider two initial mass functions (IMFs)—a Salpeter IMF, and a mass function with a characteristic mass of $10 M_{\odot}$. Previous observations suggest that the carbon abundances of red giants are altered during red-giant branch evolution due to mixing of their convective outer layers, resulting in a reduction of the observed carbon-abundance ratios. Thus, in order to derive more accurate estimates of CEMP frequencies for stars in the Milky Way, it is preferable to make use of SDSS/SEGUE main-sequence turnoff stars, which are not expected to experience significant dilution. However, because of the difficulty of identifying moderately carbon-enhanced stars ($+0.7 < [C/Fe] < +1.5$) among warm, metal-poor turnoff stars, owing to their much weaker CH *G*-bands, we derive a correction function to compensate for the resulting undercounts of CEMP stars. These comparisons indicate good agreement between the observed CEMP frequencies for stars with $[Fe/H] > -1.5$ and a Salpeter IMF, but not with an IMF having a higher characteristic mass. Thus, while the adopted AGB model works well for low-mass progenitor stars, it does not do so for high-mass progenitors. Our results imply that the IMF shifted from high- to low-mass dominated in the early history of the Milky Way, which appears to have occurred at a “chemical time” between $[Fe/H] = -2.5$ and $[Fe/H] = -1.5$. The corrected CEMP frequency for the turnoff stars with $[Fe/H] < -3.0$ is much higher than the AGB model prediction from the high-mass IMF, supporting the previous assertion that one or more additional mechanisms, not associated with AGB stars, are required for the production of carbon-rich material below $[Fe/H] = -3.0$.

Subject headings: Method: data analysis – technique: imaging spectroscopy – Galaxy: halo – stars: abundances – stars: AGB – stars: carbon

1. INTRODUCTION

Numerous spectroscopic studies of metal-poor ($[Fe/H] < -1.0$) candidates identified by the HK survey (Beers et al. 1985, 1992) and the Hamburg/ESO Survey (HES; Wisotzki et al. 1996; Christlieb et al. 2001, 2008; Christlieb 2003) have revealed that the frequency of carbon-enhanced stars increases strongly with decreasing $[Fe/H]$. These stars, now known as carbon-enhanced metal-poor (CEMP) stars, were originally defined as stars with metallicity $[Fe/H] \leq -1.0$ and carbon-to-iron ratios $[C/Fe] \geq +1.0$ (Beers & Christlieb 2005).⁶ Generally, the frequency of C-rich stars increases from a few percent at higher metallicity to on the order of 20% for $[Fe/H] < -2.0$, 30% for $[Fe/H] < -3.0$, 40% for $[Fe/H] < -3.5$, and 75% for $[Fe/H] < -4.0$ (Beers et al. 1992; Norris et al. 1997; Rossi et al. 1999; Beers & Christlieb 2005; Cohen et al. 2005; Marsteller et al. 2005; Rossi et al. 2005; Frebel et al. 2006; Lucatello et al. 2006; Norris et al. 2007; Carollo et al. 2012; Norris et al. 2013; Spite et al. 2013; Yong et al. 2013). This increasing trend of CEMP-star frequency with declining $[Fe/H]$ is again confirmed from the many thousands of CEMP stars found among the several hundred thousand stars with available spectra from the Sloan Digital Sky Survey (SDSS; Fukugita et al. 1996; Gunn et al. 1998, 2006; York et al. 2000; Stoughton et al. 2002; Abazajian et al. 2003,

2004, 2005, 2009; Pier et al. 2003; Adelman-McCarthy et al. 2006, 2007, 2008; Aihara et al. 2011; Ahn et al. 2012) and the Sloan Extension for Galactic Understanding and Exploration (SEGUE-1; Yanny et al. 2009), and SEGUE-2 (C. Rockosi et al., in preparation) as described by Lee et al. (2013).

There exist a number of subclasses within the CEMP classification, as originally defined by Beers & Christlieb (2005), which may provide direct clues to the nature of their likely progenitors. Stars in the CEMP-*s* subclass exhibit over-abundances of *s*(low)-process elements such as Ba and Sr, the CEMP-*r* subclass includes stars with enhanced *r*(apid)-process elements such as Eu, and the CEMP-*r/s* stars exhibit elemental abundance patterns associated with both the *r*-process and the *s*-process. The CEMP-no subclass exhibits no over-abundances of the neutron-capture elements.

The CEMP-*s* (and CEMP-*r/s*) subclasses of CEMP stars are the most commonly found to date; high-resolution spectroscopic studies show that around 80% of the CEMP stars are categorized as CEMP-*s* (or CEMP-*r/s*) (Aoki et al. 2007, 2008). The favored mechanism for the production of the high $[C/Fe]$ ratios found for CEMP-*s* (CEMP-*r/s*) stars is mass transfer of carbon-enhanced material from the envelope of a now-defunct asymptotic giant-branch (AGB) star to its (presently observed) binary companion (Suda et al. 2004; Herwig 2005; Komiya et al. 2007; Sneden et al. 2008; Masseron et al. 2010; Bisterzo et al. 2011, 2012). Observational evidence now exists to suggest that the CEMP-*r/s*

⁶ Different criteria, such as $[C/Fe] > +0.5$ and $[C/Fe] > +0.7$ are used by a number of studies as well; most recent work assumes $[C/Fe] > +0.7$.

stars (and other r -process-element rich stars) were enhanced in r -process elements in their natal gas clouds by previous generations of supernovae (SNe), and did not require a contribution of r -process elements from a binary companion (see Hansen et al. 2013).

The limited amount of long-term radial-velocity monitoring available for CEMP stars indicates variations for almost all of the CEMP- s stars, confirming their binary status (Lucatello et al. 2005a). In addition, the CEMP- s stars are mostly, though not exclusively (e.g., Norris et al. 2013 and references therein), found among metal-poor stars with $[\text{Fe}/\text{H}] > -3.0$. On the other hand, CEMP-no stars are found most commonly among the extremely metal-poor (EMP) stars, with $[\text{Fe}/\text{H}] < -3.0$ (Aoki et al. 2007; Norris et al. 2013). Existing radial-velocity monitoring of these objects indicates that they are found in binary systems no more frequently than other metal-poor stars (T. Hansen et al., in preparation). Norris et al. (2013) found no CEMP- s stars among 18 CEMP stars with $[\text{C}/\text{Fe}] \geq +0.7$ and $[\text{Fe}/\text{H}] < -3.1$, as well as no discernible variations of their radial velocities.

Although there is general consensus on the origin of CEMP- s stars, the likely progenitor or progenitors of the CEMP-no stars are still under discussion. Suggested models include massive, rapidly rotating, mega metal-poor (MMP; $[\text{Fe}/\text{H}] < -6.0$) stars, which produce large amounts of C, N, and O due to distinctive internal burning and mixing episodes (Meynet et al. 2006, 2010; Chiappini 2013), and faint (low-energy) SNe associated with the first generations of stars, which experience extensive mixing and fallback during their explosions, and eject large amounts of C and O, but not heavier metals (Umeda & Nomoto 2003, 2005; Tominaga et al. 2007, 2013; Ito et al. 2009, 2013; Nomoto et al. 2013). Nevertheless, the origin of the CEMP-no star phenomenon is yet to be fully resolved (see Norris et al. 2013, which summarizes other possible progenitors of the C-rich stars).

Previous authors have attempted to understand the large fractions of CEMP stars at low metallicity, as well as the different subclasses of the CEMP stars, by invoking AGB models with different masses. Furthermore, there have been several efforts to constrain the form of the early initial mass function (IMF) by reproducing the observed frequencies of CEMP stars, as well as the number ratios of the different CEMP subclasses. Abia et al. (2001), for example, claimed that the large number of carbon-enhanced stars found among stars of very low metallicity could be accounted for if the IMF in the early history of the Galaxy was dominated by higher mass stars. Lucatello et al. (2005b) and Komiya et al. (2007) utilized population-synthesis models with an IMF biased towards massive stars to compare with the fractions of observed CEMP stars, and concluded that an IMF comprising a larger number of intermediate- to high-mass stars could reproduce the larger fraction of the CEMP stars among metal-poor stars ($[\text{Fe}/\text{H}] < -2.5$) better than the present-day (Salpeter) IMF. Recently, Suda et al. (2013) made use of the number ratios of CEMP/EMP, CEMP-no/CEMP, and NEMP/CEMP giant stars (where NEMP stands for nitrogen-enhanced metal-poor) from the Stellar Abundances for Galactic Archeology (SAGA; Suda et al. 2008) database to constrain the parameters in their binary population-synthesis model. They considered several IMFs, and proposed that the IMF changed from high-mass dominated in the early Galaxy to low-mass ($M < 0.8 M_{\odot}$) dominated at present, and that this transition occurred around a metallicity of $[\text{Fe}/\text{H}] \sim -2.0$.

The above studies carried out comparisons of the CEMP

fractions derived from small samples of stars comprising mostly giants. However, observational evidence indicates that the C-rich material at the surface of a giant could be easily depleted by extra mixing of CNO-processed material from its interior during the so-called first dredge-up episode (Spite et al. 2005, 2006; Lucatello et al. 2006; Aoki et al. 2007). It is also known that more luminous red giant-branch (RGB) stars are more affected by such mixing (Spite et al. 2005, 2006). Therefore, if such mixing does occur, the overall CEMP frequencies as estimated from giants are expected to be a lower limit.

In order to avoid this complication, the best way forward would appear to be comparing model predictions with the observed CEMP frequencies based on unevolved stars, such as dwarfs or main-sequence turnoff stars. The current CEMP stars that have been studied with high-resolution spectroscopy are mostly giants (for which it is simpler to obtain high S/N spectra, due to their relative brightness and moderate temperatures, which allows for lines of interest to be measured with less uncertainty). The numbers of observed dwarf and turnoff stars with similar observations are in any case too small to derive statistically meaningful results for different subclasses of CEMP stars.

In this study, we make use of stars with available carbon-to-iron ratios ($[\text{C}/\text{Fe}]$) and $[\text{Fe}/\text{H}]$, based on medium-resolution ($R \sim 2000$) spectroscopy obtained during the course of the SDSS, SEGUE-1, and SEGUE-2, in order to derive accurate frequencies of CEMP stars among giants and turnoff stars as a function of $[\text{Fe}/\text{H}]$. The derived CEMP frequencies are then compared with the predictions from AGB binary-synthesis models that employ the two different IMFs explored by Suda et al. (2013). The results of these comparisons should provide more stringent constraints on the IMF of the Milky Way, and clues to the existence of progenitors *other than AGB stars* that are capable of producing large amounts of carbon-enhanced material in the early universe.

This paper is outlined as follows. In Section 2, we describe the selection criteria used to assemble the sample for this study. Section 3 presents and discusses results of the comparison of the CEMP frequencies for giants and main-sequence turnoff stars with the binary-synthesis model predictions, and describes a procedure for correcting the anticipated undercounts of CEMP stars among warm, metal-poor turnoff stars. Our conclusions are presented in Section 4.

2. CARBON-ENHANCED SDSS/SEGUE STARS

The SDSS, SEGUE-1, and SEGUE-2 surveys have produced an unprecedented number of high-quality medium-resolution stellar spectra, covering stars in various evolutionary stages, and spanning a wide range of metallicity ($-4.0 < [\text{Fe}/\text{H}] < +0.5$). A total of about 600,000 stars are potentially suitable for examination of the properties of the Milky Way's stellar populations. The resolving power of the spectra is $R \sim 2000$, over the wavelength range 3820–9100 Å. Below we simply refer to these stars (spectra) as SDSS/SEGUE stars (spectra). Accurate estimates of the atmospheric parameters for most of the SDSS/SEGUE stars are derived using the latest version of the SEGUE Stellar Parameter Pipeline (SSPP; Lee et al. 2008a, 2008b, 2011; Allende Prieto et al. 2008; Smolinski et al. 2011). The typical external errors obtained by the SSPP are 180 K for T_{eff} , 0.24 dex for $\log g$, and 0.23 dex for $[\text{Fe}/\text{H}]$, respectively (Smolinski et al. 2011). In addition, estimates of the carbonicity, $[\text{C}/\text{Fe}]$, is obtained following the prescription of Lee et al. (2013), for stars with $4400 \leq$

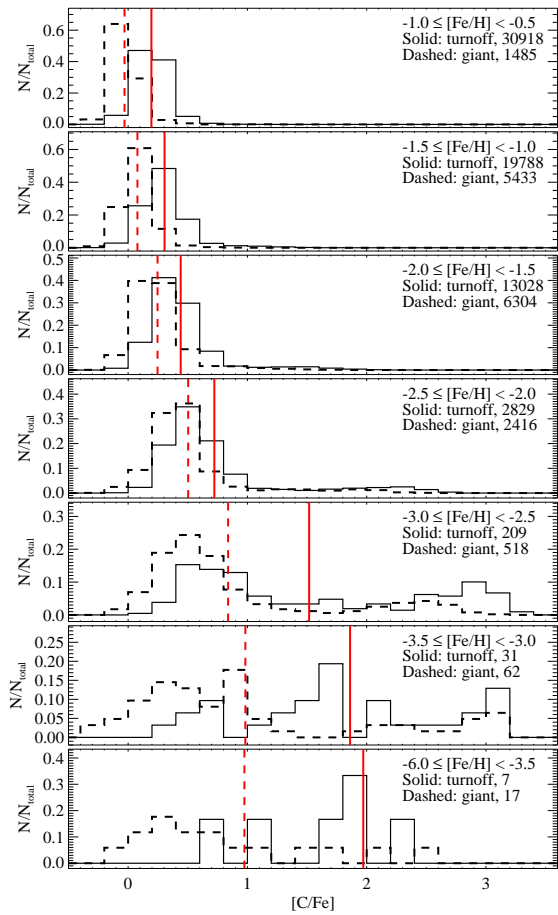


FIG. 1.— Distribution of $[C/Fe]$ for SDSS/SEGUE stars over different ranges of $[Fe/H]$, decreasing from the upper to lower panels. Main-sequence turnoff stars are shown as solid histograms; giants are shown as dashed histograms. The metallicity range in each panel is indicated by the legends, along with the total number of stars shown in the histograms. The solid and dashed red vertical lines indicate the mean values of $[C/Fe]$ for the turnoff stars and giants, respectively. On average, the turnoff stars exhibit higher carbon enhancement than the giants.

$T_{\text{eff}} \leq 6700$ K, where accurate $[C/Fe]$ can be determined. As reported by Lee et al., uncertainties in the determination of $[C/Fe]$ are smaller than 0.35 dex for SDSS/SEGUE spectra with $S/N \geq 15 \text{ \AA}^{-1}$.

In order to derive reliable frequencies of the CEMP stars among the field stellar populations, we follow the selection criteria of Lee et al. (2013). Briefly, we first exclude all stars located in the directions of known open and globular clusters. For stars that were observed more than once, we keep only the parameters derived from the highest S/N spectrum. We then restrict the sample to stars with spectra having $S/N \geq 20 \text{ \AA}^{-1}$, effective temperatures in the range $4400 \text{ K} \leq T_{\text{eff}} \leq 6700 \text{ K}$, and metallicities in the range $-4.0 \leq [Fe/H] \leq +0.5$, so that our estimates of $[C/Fe]$ are as reliable as possible.

We then visually inspect each spectrum with $[Fe/H] \leq -2.0$, in order to reject spectra such as cool white dwarfs, or those with emission-line features in the cores of their Ca II lines, or other spectral defects that could lead to spurious determinations of metallicity by the SSPP. Additionally, we visually examine the spectra for all stars with $[C/Fe] \geq +0.7$, and exclude stars with poor estimates of $[Fe/H]$ and/or $[C/Fe]$. Following Lee et al., for the purpose of deriving the CEMP frequencies we do not include stars with $[C/Fe] \geq +0.7$ and indication of upper limit estimate, and consider these stars to have unknown

carbon status. By application of the above procedures, we are left with a sample of about 247,350 stars.

For the purpose of our analysis, we consider stars with $4400 \text{ K} \leq T_{\text{eff}} \leq 5600 \text{ K}$ and $1.0 \leq \log g < 3.2$ as giants, and stars with $5600 \text{ K} \leq T_{\text{eff}} \leq 6600 \text{ K}$ and $3.2 \leq \log g < 4.5$ as main-sequence turnoff stars. The distance to each star is estimated following the prescriptions of Beers et al. (2000, 2012), which obtains photometric distance estimates with errors on the order of 10%–20%.

Note that we have added stars to our sample from Table 1 of Yong et al. (2013), and one object from Caffau et al. (2011), with determinations based on high-resolution spectroscopic analyses, in order to increase the number of stars with $[Fe/H] < -3.0$. This results in better number statistics for the calculation of the CEMP frequencies in the extremely and ultra metal-poor regime.

3. RESULTS AND DISCUSSION

3.1. Differences in Average $[C/Fe]$ Between Giants and Turnoff Stars

Figure 1 shows the distribution of $[C/Fe]$ for SDSS/SEGUE stars in various bins of metallicity, decreasing from the upper to lower panels. Main-sequence turnoff stars are shown as solid histograms; giants are shown as dashed histograms. Inspection of this figure reveals that the overall distribution of $[C/Fe]$ gradually shifts (for both turnoff stars and giants) to higher $[C/Fe]$ with decreasing $[Fe/H]$, with a tail extending toward higher $[C/Fe]$ appearing as the metallicity decreases. As the metallicity decreases below $[Fe/H] = -3.0$, this trend continues for the turnoff stars, but it is not as evident for the giants.

Another interesting feature seen in Figure 1 is that, for $[Fe/H] < -3.0$, the turnoff stars are distributed over a wide range of $[C/Fe]$, whereas the giants are mostly concentrated in the region of $[C/Fe] < +1.0$. The red vertical lines in Figure 1 indicate the mean values of $[C/Fe]$ for the turnoff stars (solid line) and giants (dashed line), respectively. On average, the giants appear to exhibit lower carbonicity (by about 0.2 dex) than the turnoff stars, down to $[Fe/H] = -2.5$. The mean value of $[C/Fe]$ appears to increase with decreasing metallicity, as also found by Carollo et al. (2012, their Figure 11). They reported that the degree of carbon enhancement significantly increased from $[C/Fe] \sim +1.0$ at $[Fe/H] = -1.5$ to $[C/Fe] \sim +1.7$ at $[Fe/H] = -2.7$, somewhat higher than our values (it should be noted that a different sample of stars, as well as a different method for determination of $[C/Fe]$, were employed by these authors).

The difference in the distribution of $[C/Fe]$ between the turnoff stars and the giants may be explained by the different masses of the convective envelopes between the two evolutionary stages. Because a giant has a much larger convective envelope, its surface material experiences more mixing, leading to reduction of the carbonicity. On the other hand, the turnoff stars have shallower convective envelopes, so that their surface abundances may not be expected to greatly change. As a result, the overall carbon abundance for the turnoff population is expected to be higher than that of the giant population, even if they were born with the same initial carbon abundance.

Bonifacio et al. (2009) also noted a difference in the mean $[C/Fe]$ between giants and turnoff stars of similar metallicities, finding a difference of about 0.2 dex (giants being lower) for stars with $[Fe/H] < -2.5$. They argued that this difference

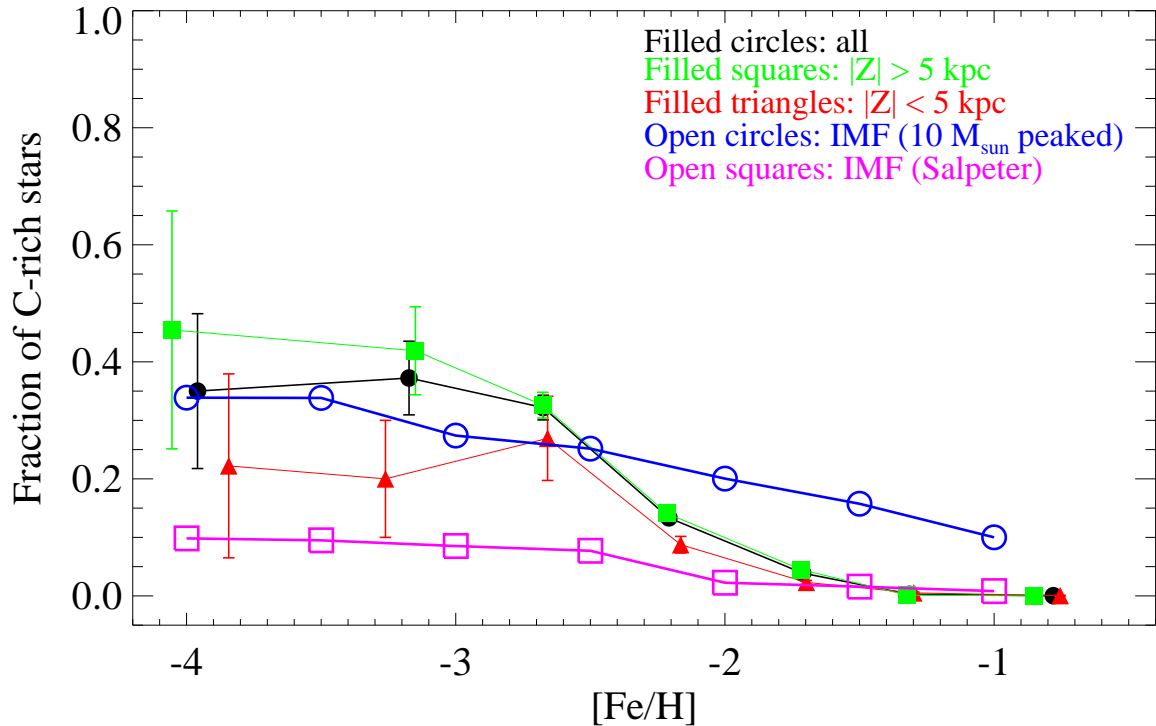


FIG. 2.— Differential frequencies of C-rich giants (defined as stars with $4400 \text{ K} \leq T_{\text{eff}} \leq 5600 \text{ K}$ and $1.0 \leq \log g < 3.2$) as a function of $[\text{Fe}/\text{H}]$. Bin sizes of 0.5 dex in $[\text{Fe}/\text{H}]$ are used for stars with $[\text{Fe}/\text{H}] > -3.5$; a single bin for stars with $[\text{Fe}/\text{H}] < -3.5$ is used. Filled circles show the derived frequencies of the CEMP stars for all giants, while the filled squares represent the subsample of CEMP stars for giants located more than 5 kpc from the Galactic plane, $|Z| > 5 \text{ kpc}$. The filled triangles indicate stars located closer to the plane, with $|Z| < 5 \text{ kpc}$. The prediction of the expected CEMP frequencies as a function of $[\text{Fe}/\text{H}]$, based on an AGB nucleosynthesis model with IMF peaked at $10 M_{\odot}$, is indicated by the open circles, while the open squares denote the prediction assuming a Salpeter IMF. Error bars are based on Poisson statistics.

arises because the giants suffer from extra mixing due to first dredge-up, and have their surface carbon abundance reduced. They also suggested the stellar models employed in the analysis could contribute to this discrepancy; they found a smaller difference between the giants and turnoff stars when deriving $[\text{C}/\text{Fe}]$ from a 3D, rather than a 1D model atmosphere.

3.2. Comparison with Model Predictions for the Frequency of C-rich Giants

The black filled circles in Figure 2 represent our derived differential frequencies for C-rich giants as a function of $[\text{Fe}/\text{H}]$. From inspection of this figure, it appears that the CEMP frequencies do not increase for $[\text{Fe}/\text{H}] < -2.5$, but rather, remain relatively constant, in contrast to the results of previous studies. As discussed by Spite et al. (2005, 2006), Lucatello et al. (2006), and Aoki et al. (2007), this may be in part due to CN-processing, which converts carbon to nitrogen at the bottom of a star’s convection zone, and in turn reduces the carbon abundance in the envelope at the time of first dredge-up. Whether or not a giant experiences such mixing can be identified by measuring its $^{12}\text{C}/^{13}\text{C}$ or $[\text{C}/\text{N}]$ ratios, as both will be lower for an object that has gone through such an event. Unfortunately, these ratios are difficult to assess from the SDSS/SEGUE spectra over the full range of metallicities we consider. In the metallicity regime of $[\text{Fe}/\text{H}] > -1.5$, our derived CEMP frequencies of $\sim 1\%$ agree with the previously claimed fraction of classical CH or Ba stars in the solar neighborhood (Luck & Bond 1991).

Regarding the effect of the first dredge-up, it is worth mentioning the following arguments from a theoretical point of view. According to Suda et al. (2004), first dredge-up might not play a significant role in decreasing the carbon abun-

dance on the surface of a giant, based on an $0.8 M_{\odot}$ model for HE 0107-5240 (a CEMP-no star with $[\text{Fe}/\text{H}] = -5.3$; Christlieb et al. 2002). They examined the effect of the first dredge-up following the accretion of C- and O-rich matter onto the star (here assuming an AGB mass-transfer scenario), and found that if its envelope is significantly C-rich ($[\text{C}/\text{Fe}] \gg +1.0$), then after first dredge-up the surface carbon abundance changed little. This is because the surface carbon abundance is too large ($[\text{C}/\text{H}] \sim -1$) prior to the dredge-up to be significantly depleted by the relatively small amount of matter in the hydrogen-burning shell, $M < 0.02 M_{\odot}$. Even in cases of EMP stars for which the initial carbon abundance is small, Suda & Fujimoto (2010) showed that the effect of the first dredge-up is also limited, due to the shallower convective envelopes in metal-poor (as compared to metal-rich) stars. According to their model calculation, the change of the CNO abundance before and after the first dredge-up was on the order of one percent. Therefore, they did not notice a large impact on the surface carbon abundances after first dredge-up for stars with $[\text{Fe}/\text{H}] < -2.3$.

The blue open circles in Figure 2 are the predicted frequencies of CEMP giants, as a function of metallicity, from AGB binary-synthesis models with an IMF peaked at $10 M_{\odot}$, while the open squares are the predicted frequencies from models using a Salpeter IMF, adopted from Suda et al. (2013). In their model, they included a mechanism referred to as “pulsation-driven mass loss” (Wood 2011), which was argued to suppress the previously predicted over-production of NEMP stars by Izzard et al. (2009) and Pols et al. (2012). It appears that the predicted CEMP frequencies for the high-mass dominated IMF are in relatively good agreement with the observed CEMP giant frequencies for $[\text{Fe}/\text{H}] < -2.5$, but the model

predicts too many C-rich stars above $[\text{Fe}/\text{H}] = -2.5$. The predicted CEMP frequencies from a Salpeter IMF are in good agreement with our derived frequencies for the metal-rich region ($[\text{Fe}/\text{H}] > -1.5$), while the predicted CEMP frequencies are far too low for stars with $[\text{Fe}/\text{H}] < -2.5$.

These are similar results to those found by Suda et al. (2013), who used the giants in the SAGA database to compare the observed CEMP frequencies with their model predictions. One of the reasons that Suda et al. (2013) employed giants to derive the CEMP frequency is that one can ignore effects such as atomic diffusion, which can alter the surface abundances of dwarfs and turnoff stars more significantly than in giants (e.g., Richard et al. 2002a,b; Korn et al. 2007; Lind et al. 2008). However, our derived frequencies show a much better agreement for the Salpeter IMF in the metallicity region $[\text{Fe}/\text{H}] > -1.5$. In the study of Suda et al. (2013), the model-predicted frequency of the CEMP stars above $[\text{Fe}/\text{H}] = -2.0$ was not well-constrained, most likely due to the selection biases associated with the assembly of their sample from previous high-resolution spectroscopic studies (which tended to emphasize the more metal-poor and/or carbon-enhanced stars). In contrast, the good agreement of the frequencies calculated from our considerably less-biased SDSS/SEGUE sample with the model prediction for $[\text{Fe}/\text{H}] > -1.5$ suggests that the AGB binary-synthesis model with a Salpeter mass function used by Suda et al. (2013) works well, at least in this metallicity regime.

Based on the results from the comparisons of the observed CEMP frequencies with model predictions from the two different IMFs, we conjecture that, for very low-metallicity ($[\text{Fe}/\text{H}] < -2.5$) stars, the distribution of the stellar masses was dominated by rather massive stars ($\sim 10 M_{\odot}$ or higher), while for the relatively more metal-rich stars ($[\text{Fe}/\text{H}] > -1.5$), it appears that the IMF did not much differ from a Salpeter IMF, which is biased towards low-mass progenitor stars ($M < 0.8 M_{\odot}$). As previously claimed by Suda et al. (2013), our results also support the idea that there must exist a shift in the IMF from a high-mass dominated to low-mass dominated form in the early history of the Milky Way, corresponding to a “chemical time” between $[\text{Fe}/\text{H}] = -2.5$ and $[\text{Fe}/\text{H}] = -1.5$.

By way of comparison, the binary population-synthesis model of Izzard et al. (2009) was able to reproduce the ratio of NEMP to very metal-poor (VMP; $[\text{Fe}/\text{H}] < -2.0$) stars (that is, C and N normal stars) *without* introducing an IMF dominated by higher mass stars, but not the high frequency of the CEMP stars. Pols et al. (2012) also argued, by comparing the observed number ratio of NEMP to CEMP stars with their model predictions, that they could derive a similar number ratio from a Salpeter IMF, and ruled out an IMF peaked at $10 M_{\odot}$ claimed by Komiya et al. (2007).

3.3. Behavior of Derived CEMP Frequencies with Distance from the Galactic Plane

Another interesting result emerges when one partitions the giant sample based on distance from the Galactic plane. The green squares in Figure 2 are the CEMP frequencies for giants with distances from the Galactic mid-plane ($|Z|$) larger than 5 kpc, whereas the red triangles represent frequencies based on those with $|Z| < 5$ kpc.⁷ The figure clearly indicates that the more distant halo giants exhibit higher frequencies of C-rich stars, while the stars closer to the Galactic plane tend to

⁷ A more quantitative analysis of the variation of CEMP frequencies with $|Z|$ will be considered in an upcoming paper of this series.

have lower frequencies of C-rich stars. This same trend with vertical distance was hinted at (due to small number statistics) in Frebel et al. (2006), and strongly confirmed in the much larger sample of SDSS/SEGUE calibration stars by Carollo et al. (2012). Carollo et al. argued that this result was likely due to the fact that the outer-halo population has about twice the frequency of CEMP stars, at a given low metallicity, as the inner-halo population.

A few possible reasons for the observed differences in the CEMP frequencies between the two spatial regions might be suggested within the context of the AGB model predictions. First, the progenitors of the inner-halo population (which dominates for $|Z| < 5$ kpc) and the outer-halo population (which, at $|Z| > 5$ kpc, includes more outer-halo stars) might have formed their stars at different times, with different IMFs. Because the outer-halo population has more CEMP stars than the model prediction for $[\text{Fe}/\text{H}] < -2.5$, it is possible that the outer-halo population might have had an IMF with more intermediate-mass stars than considered by the model. On the other hand, since the CEMP frequencies of the inner-halo stars are lower than the model estimate, the inner-halo population might have had an IMF with less intermediate-mass stars than the proposed IMF. Related ideas are discussed by Tumlinson et al. (2007).

Another possibility is that Suda et al. (2013) assumed that all CEMP stars, including CEMP-no objects, formed from the AGB binary scenario. If there were to exist other channels of carbon production at $[\text{Fe}/\text{H}] < -2.5$, such as faint SNe or rapidly rotating massive stars (producing CEMP-no stars in the subsequent generation), as suggested by several studies, we then might expect larger frequencies of CEMP stars than the AGB binary-synthesis model prediction (as seen in Figure 2), even if the carbon dilution of the giants due to extra mixing is taken into account. A more detailed discussion of this is provided below.

In any event, the frequency difference we find can be understood (as argued by Carollo et al. 2012) as the result of a change in the dominant population with distance above the plane, from the inner-halo population to the outer-halo population. Carollo et al. further argued that the inner halo is dominated by stars with modest carbon enhancement ($[\text{C}/\text{Fe}] \sim +0.5$), while the outer halo has a greater portion of stars with large carbon enhancements ($[\text{C}/\text{Fe}] \sim +2.0$), although considerable overlap still exists. They interpreted these results, as well as the increase in the global frequency of CEMP stars with distance from the Galactic plane, as evidence for the possible presence of additional astrophysical sources of carbon, beyond AGB production alone, associated with the progenitors of the outer-halo stars.

It is difficult to separate CEMP-*s* and CEMP-no stars from our medium-resolution SDSS/SEGUE spectra, but determination of the ratio of CEMP-*s*/CEMP-no for stars in the inner- and outer-halo populations, based on high-resolution spectroscopy, will provide not only very strong constraints on the binary-synthesis model, but clues to the origin of the different CEMP frequencies between the inner- and outer-halo populations.

3.4. Correcting the CEMP Frequencies for Main-Sequence Turnoff Stars

Above we have compared the derived CEMP frequencies from our sample of giants with the predicted CEMP frequencies from AGB binary-synthesis models by Suda et al. (2013). However, as previously mentioned, observations suggest that

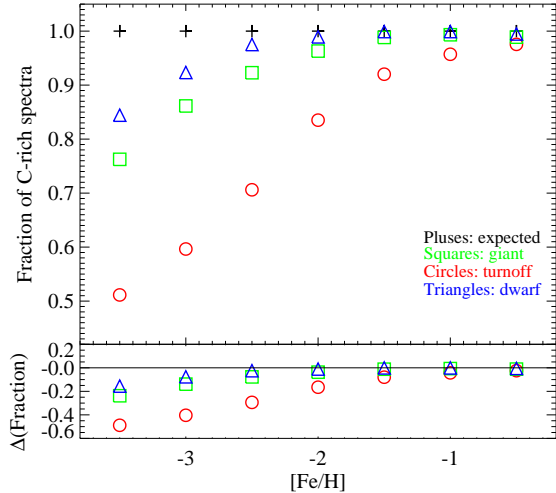


FIG. 3.— Fractions of noise-added synthetic spectra with $[C/Fe] < +0.7$ estimated by the SSPP among model spectra with mild carbon enhancements, in the range $+0.75 \leq [C/Fe] \leq +1.25$. The plus signs are the actual expected fractions (set for convenience to unity). The green squares indicate the calculated fraction of CEMP stars for giants, defined as models with parameters $4500 \text{ K} \leq T_{\text{eff}} \leq 5500 \text{ K}$ and $1.0 \leq \log g \leq 3.0$. The red circles are the calculated frequencies for turnoff stars, defined as models satisfying with $5750 \text{ K} \leq T_{\text{eff}} \leq 6500 \text{ K}$ and $3.5 \leq \log g \leq 4.0$. The blue triangles represent the frequencies for main-sequence dwarfs, defined to have $4500 \text{ K} \leq T_{\text{eff}} \leq 5500 \text{ K}$ and $4.5 \leq \log g \leq 5.0$. The bottom panel shows the distribution of residuals in the fractions for the three populations.

a giant can suffer from dilution of the carbon-rich material in its envelope by mixing during the first dredge-up event, resulting in a lower overall carbon abundance and (as a population) lower frequencies of CEMP stars. Absent such dilution, we would expect that the actual frequencies of CEMP stars among giants would be higher than shown in Figure 2.

Stars near the main-sequence turnoff region do not experience dredge-up episodes; rather, they preserve unpolluted material on their surfaces. It might be possible that their surface abundances could be affected by atomic diffusion, but because the impact on the carbon abundance is not well known, we do not take this concern into consideration in this study. Thus, we expect that one could obtain a more valid estimate of the frequencies of CEMP stars in a given population by making this evaluation using main-sequence turnoff stars. Since turnoff stars evolve quickly into giants during their evolution, we might expect that the frequencies of CEMP stars inferred from stars near the main-sequence turnoff should be the same as for giants that have not yet mixed carbon-depleted material into their envelopes. Therefore, it is desirable to compare the predictions from the models to the frequencies of CEMP stars derived from the turnoff stars.

However, additional complications exist. The stars located near the main-sequence turnoff are relatively warmer than the red giants, and as a result, for a given carbon abundance, the molecular CH G -band feature becomes significantly weaker. To make matters more difficult, at low metallicity (assuming carbon is not enriched) a star’s CH G -band will also become lower in strength. Even with high-resolution spectroscopy Aoki et al. (2013) noted that, although they were able to detect the CH G -band for a star with $[C/Fe] \geq +1.5$ and $[Fe/H] \sim -3.0$ at $T_{\text{eff}} \sim 6000 \text{ K}$, they failed to measure the CH G -band for $[C/Fe] < +1.5$ in their sample of very metal-poor stars. These effects become even more prevalent for medium-resolution spectra, hence the calculated CEMP frequencies obtained from the turnoff stars may also be lower than the

actual values.

In order to address this difficulty, and to provide a check on just how many C-rich halo stars may have been misclassified as C-normal objects ($[C/Fe] < +0.7$) for stars around the turnoff region, we have performed the following experiment. Following the prescription by Lee et al. (2013), we inject artificial noise (with characteristics similar to that for a typical SDSS/SEGUE spectrum) into the grid of synthetic spectra that are used to estimate $[C/Fe]$. The noise-added synthetic spectra have $S/N = 40, 45, \text{ and } 50$, which are typical of the quality of the SDSS/SEGUE spectra in our study with $|Z| < 5 \text{ kpc}$ (justification for this choice is provided below). At each S/N there are 25 different realizations. These spectra are processed through the SSPP to determine estimates of $[C/Fe]$. With the measured $[C/Fe]$ in hand, we then derive the CEMP frequencies of the spectra, as a function of $[Fe/H]$, which have an *estimated* $[C/Fe]$ less than $+0.7$ among the spectra with $+0.75 \leq [C/Fe] \leq +1.25$ for giants, turnoff stars, and dwarf stars (note that we employ discrete $[C/Fe]$ values, $+0.75, +1.0, \text{ and } +1.25$ for the synthetic spectra). For the purpose of this exercise, we define giants as models with parameters in the ranges $4500 \text{ K} \leq T_{\text{eff}} \leq 5500 \text{ K}$ and $1.0 \leq \log g \leq 3.0$, turnoff stars for $5750 \text{ K} \leq T_{\text{eff}} \leq 6500 \text{ K}$ and $3.5 \leq \log g \leq 4.0$, and dwarfs for $4500 \text{ K} \leq T_{\text{eff}} \leq 5500 \text{ K}$ and $4.5 \leq \log g \leq 5.0$.

Figure 3 shows the results of this experiment. The plus signs represent the actual frequencies of CEMP stars, which are set to 1.0. The green squares indicate giants, the red circles the turnoff stars, and the blue triangles the dwarfs. The bottom plot exhibits the residuals in the derived fractions (simply $1 - \text{the fractions}$) in each category. Inspection of this figure reveals that some of the C-rich dwarfs and giants start to be classified as C-normal ($[C/Fe] < +0.7$) from around $[Fe/H] < -2.0$; the number of the misclassified stars slowly increases with decreasing metallicity. By way of comparison, the C-rich turnoff stars begin to be misclassified as C-normal stars as metallicity drops below $[Fe/H] = -1.0$; this misclassification rapidly increases with declining metallicity, as expected.

We now derive a correction function for capturing the “true” CEMP frequency, as a function of $[Fe/H]$, for the SDSS/SEGUE turnoff stars, based on the results of the test carried out above. We then use this correction function to adjust the frequency calculation, among the stars with $+0.7 \leq [C/Fe] < +1.5$, taking the “missing” C-rich stars into account.

3.5. Comparison with Model Predictions for the Frequencies of C-rich Turnoff Stars

Since the giants are more luminous than the turnoff stars, they can probe to greater distances in the Galaxy. This increases the likelihood of introducing a greater number of giants than turnoff stars into a magnitude-limited sample (the frequency of giants can also be influenced by the luminosity function of the halo field stars, as well as by shifts in the mix of stellar populations between the nearby and more distant halo stars). This possible population transition has already been noted in Figure 2, and discussed in detail in the previous section. Thus, in order to make sure we are sampling the giants and turnoff stars in similar regions of the Galaxy, we restrict our considerations to the stars with $|Z| < 5 \text{ kpc}$ for the calculation of the CEMP frequencies.

Figure 4 shows the differential frequencies of C-rich stars for main-sequence turnoff stars, as a function of $[Fe/H]$, as red open triangles; the corrected frequencies are indicated as green filled triangles. The blue open circles represent the

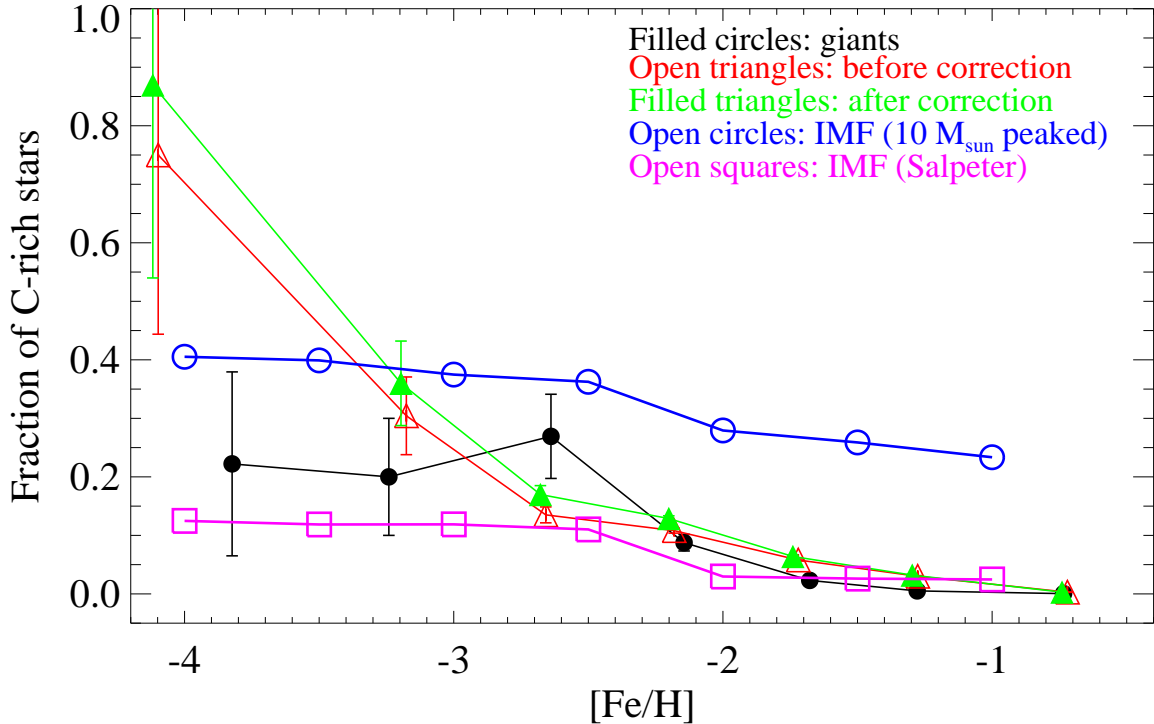


FIG. 4.— Differential frequencies of C-rich main-sequence turnoff stars, as a function of $[\text{Fe}/\text{H}]$. The metallicity bins are the same as in Figure 2. Only stars located at $|Z| < 5$ kpc are considered. The red open triangles represent the “as-observed” frequencies for the subsample of turnoff stars, defined as stars with parameters in the range $5600 \text{ K} \leq T_{\text{eff}} \leq 6600 \text{ K}$ and $3.2 \leq \log g \leq 4.5$, while the green filled triangles indicate the corrected CEMP frequencies for this same sample (see text). The open circles and squares are the AGB binary-synthesis model predictions for the two different IMFs. For comparison, the frequencies of the CEMP giants with $|Z| < 5$ kpc are plotted as filled circles.

predicted turnoff CEMP frequencies from an AGB binary-synthesis model with an IMF peaked at $10 M_{\odot}$, while the magenta open squares indicates the prediction obtained using a Salpeter IMF. For comparison, the filled black circles are the frequencies from the giants with $|Z| < 5$ kpc given in Figure 2. The behavior seen in this figure is consistent with our expectations, in that the CEMP frequencies for the giants are lower than that for the turnoff sample, at least at the lowest metallicities. Note that the corrected CEMP frequencies for the turnoff stars are, on average, higher than the uncorrected frequencies, by about 5%. The figure also shows that the models produce higher CEMP frequencies for the turnoff stars than for the giants for both IMFs (compare with Figure 2), which at least qualitatively agrees with the observations. The small difference in the model-predicted CEMP frequencies between the giants and turnoff stars (Figures 2 and 4) may arise from the difference in the mass of the convective envelope; a star that evolves to the giant stage has a much deeper convective zone, and hence more effective dilution, resulting in lower CEMP frequencies derived for the giants.

Our derived CEMP frequencies from the distance-restricted turnoff sample appears to be in good agreement with the model prediction based on a Salpeter IMF (magenta open squares), down to $[\text{Fe}/\text{H}] = -2.5$. This reaffirms that the AGB model for progenitor stars in the low-mass range works well. However, the model estimate of the CEMP frequency does not reproduce the observed frequencies for $[\text{Fe}/\text{H}] < -2.5$. Unlike the case for the giants (Figure 2), the observed CEMP frequencies from our turnoff sample do not agree with the model estimation from the top-heavy IMF for $[\text{Fe}/\text{H}] < -2.5$ at all, as these remain roughly flat instead of growing dramatically with decreasing metallicity.

One reason for the large discrepancy between the model estimates and the observed frequencies of CEMP stars may be uncertainties of the model parameters adopted for producing carbon in the AGB star, and subsequent processes that enrich (or deplete) the envelope with carbon. Below we discuss known sources of uncertainty associated with the AGB binary-synthesis model, which may result in changes of the predicted carbon abundance of the secondary star.

Most AGB stars in the mass range of $\sim 1\text{--}8 M_{\odot}$ can produce carbon, but whether or not they develop carbon-enriched envelopes depends on the efficiency of the third dredge-up (TDU) and helium-flash driven deep mixing (He-FDDM; Fujimoto et al. 1990, 2000)⁸ events for $[\text{Fe}/\text{H}] < -2.5$. At present, it is not fully understood how such episodes depend on the mass and metallicity of an AGB star.

For example, Lau et al. (2009) claimed, in a study of the evolution of AGB stars with metallicity between $Z = 10^{-8}$ and 10^{-4} , that the He-FDDM did not take place for $Z > 10^{-5}$ independent of the mass of a star, and that this event did not occur for a star with $M > 2 M_{\odot}$, regardless of its metallicity. However, Suda & Fujimoto (2010) found, from an extensive set of stellar evolution models, that the He-FDDM event occurred for a star with $M \leq 3 M_{\odot}$ for zero metallicity, while it occurred for a star with $M \leq 2 M_{\odot}$ for $-5 \leq [\text{Fe}/\text{H}] \leq -3$. They also found that the TDU episode was restricted to a mass range of $M \sim 1.5\text{--}5 M_{\odot}$ for $[\text{Fe}/\text{H}] = -3.0$, and that this mass range becomes smaller as the metallicity decreases.

In the adopted models from Suda et al. (2013), the increasing fractions of CEMP stars comes from the He-FDDM, which can enhance the surface carbon abundance by a fac-

⁸ Often referred to as a dual shell flash or carbon ingestion episode.

tor of 10, from $[C/H] \sim -1$ to $+0$, regardless of the initial metallicity of the models, for stars with masses of $0.8\text{--}3 M_{\odot}$. In this view, the value of $[C/Fe]$ for the secondary component (the presently observed CEMP star) of a given binary increases with decreasing $[Fe/H]$, so that a larger fraction of CEMP stars can be achieved at lower metallicity. It is also assumed that the efficiency of the binary mass transfer and the mass-loss rates do not depend on metallicity.

In addition, among these AGB stars, the intermediate-mass ($\sim 3\text{--}8 M_{\odot}$) objects can be enriched with nitrogen by operation of the hot-bottom burning (HBB) process, which converts carbon into nitrogen by CN processing, and predicts the production of NEMP stars (Johnson et al. 2007). However, the dependency of the HBB on the mass and metallicity of an AGB star is yet not well-established.

Even taking into account the uncertainties in the parameters of the AGB models, a more plausible interpretation of our results may be the existence of additional (non-AGB) carbon-production mechanisms, as discussed in the Introduction, which result in large frequencies of CEMP stars in the metallicity regime $[Fe/H] < -3.0$. The current observations certainly favor this interpretation, since most CEMP-no stars in the Galaxy appear at $[Fe/H] < -3.0$, and these stars do not commonly exhibit the radial velocity variations that would be expected if membership in a binary system were required (as in the AGB mass-transfer scenario).

The adopted models, however, assume that all CEMP-no stars form from the AGB binary mass-transfer scenario, rather than including additional sources that have been argued are likely to be present in the early universe. According to the AGB models, low-mass ($M < 3.5 M_{\odot}$) AGB stars efficiently create s -process elements by generating extra neutrons via the $^{13}\text{C}(\alpha, n)^{16}\text{O}$ reaction, while a weak s -process (for light s -process elements) operates by $^{22}\text{Ne}(\alpha, n)^{25}\text{Mg}$ for the intermediate-mass stars. CEMP-no stars could form in the AGB mass-transfer scenario by suppressing the formation of the ^{13}C pocket for intermediate mass stars ($M > 3.5 M_{\odot}$; Suda et al. 2013). Thus, in order to preferentially produce CEMP-no stars at low metallicity and maintain the observed ratio of CEMP-no/(CEMP- s + CEMP-no), which is close to 0.5 at $[Fe/H] \sim -3.0$ (from Table 1 of Suda et al. 2013), the models have to assume that the ^{13}C pocket does not form in stars with metallicity significantly below $[Fe/H] = -2.5$.

It has also been suggested (Komiya et al. 2007) that a secondary star with an AGB primary having $0.8 M_{\odot} < M < 3.5 M_{\odot}$ could become a CEMP- s star following mass transfer, while systems that include an AGB primary with $M > 3.5 M_{\odot}$ could produce C without the enhancement of neutron-capture elements, leading to a CEMP-no star following mass transfer. However, current AGB models do not satisfactorily explain the absence of the ^{13}C pocket at low metallicities, even though this assumption has been invoked to explain the observed decreasing trend of $[Pb/Ba]$ for CEMP stars with $[Fe/H] < -2.5$ (Aoki et al. 2002; Suda et al. 2004; Barbuy et al. 2005; Cohen et al. 2006; Aoki et al. 2008). It is also significant that Ito et al. (2013) obtained a rather low upper limit on the abundance of lead ($\log \epsilon(\text{Pb}) < -0.10$) for the $[Fe/H] = -3.8$ CEMP-no star BD+44°493, while previous predictions called for $\log \epsilon(\text{Pb}) \sim +1.5$ at these low metallicities if the lead were produced by the s -process (Cohen et al. 2006).

Chemical abundances of CEMP-no stars observed with high-resolution spectroscopy (e.g., Ito et al. 2009, 2013; Norris et al. 2013) support other scenarios for significant carbon

production. Their abundance patterns are similar to the predictions from massive, rapidly rotating, MMP stars (Meynet et al. 2006, 2010) or faint SNe that experience mixing and fallback (Umeda & Nomoto 2003, 2005; Tominaga et al. 2007, 2013; Kobayashi et al. 2011; Ito et al. 2013; Nomoto et al. 2013). If such mechanisms are the dominant sources of the large amounts of carbon produced at low metallicity, these scenarios also favor an IMF that preferentially produces massive stars. In fact, one might also expect a rather abrupt “break” in the CEMP frequencies when the primary carbon sources change in nature—such a sudden change can be seen for the turnoff stars in Figure 4 below $[Fe/H] = -3.0$. Although we are not able to distinguish CEMP-no stars from CEMP- s stars in our sample, given that the majority of the CEMP-no stars are found with $[Fe/H] < -3.0$, our derived frequencies imply that non-AGB related phenomenon may be the dominant mechanisms for producing large carbon abundances at extremely low $[Fe/H]$.

Finally, we see that a similar behavior in the CEMP frequencies with $[Fe/H]$ applies to the turnoff stars with $-2.5 < [Fe/H] < -1.5$ as for the giants, suggesting that the proposed shift in an IMF occurred over this chemical interval.

4. CONCLUSIONS

We have compared our derived CEMP frequencies from the SDSS/SEGUE giant sample with that predicted by AGB binary-synthesis models with two different IMFs—a Salpeter IMF, and an IMF with a characteristic mass of $10 M_{\odot}$. Good agreement of the CEMP frequencies for $[Fe/H] > -1.5$ with the Salpeter IMF indicates that the adopted AGB model works well for low-mass progenitor stars. Qualitatively, better agreement with an IMF biased to higher-mass progenitors is found for $[Fe/H] < -2.5$, suggesting that the nature of the IMF shifted from one that is high-mass dominated in the early history of the Milky Way galaxy, to one that is now low-mass dominated. This transition appears to have occurred, in “chemical time”, between $[Fe/H] = -2.5$ and $[Fe/H] = -1.5$, as other recent studies have argued (e.g., Suda et al. 2011, 2013; Yamada et al. 2013).

As noted by other recent work, the more distant halo giants (those with $|Z| > 5$ kpc) exhibit higher frequencies of CEMP stars compared to those closer to the Galactic plane. A plausible explanation for this difference is the expected change of the dominant stellar populations from the inner-halo to the outer-halo population, coupled with the assumption that the outer-halo stars are associated with progenitors capable of producing large amounts of carbon without the accompanying production of heavy metals. Thus, one might expect that the inner-halo population harbors a higher ratio of CEMP- s /CEMP-no stars, while the opposite may apply to the outer-halo population. Tests of this hypothesis are underway (D. Carollo et al., in preparation).

The weak CH G -bands for moderately carbon-enhanced stars ($+0.7 < [C/Fe] < +1.5$) among warm, metal-poor main-sequence turnoff stars results in their likely having been undercounted by previous assessments of CEMP frequencies. We have derived a correction function to compensate for this, making use of noise-added synthetic spectra. The corrected CEMP frequencies for turnoff stars are, on average, higher by $\sim 5\%$ than with the uncorrected frequencies. Both the corrected and uncorrected CEMP frequencies derived from the turnoff sample exceed those of the giants for $[Fe/H] < -3.0$.

We have made use of main-sequence turnoff stars with $|Z| < 5$ kpc to compute more realistic CEMP frequencies than

obtained by using giants (or the combination of giants with other classes), corrected as mentioned above. For $[\text{Fe}/\text{H}] > -2.5$, our corrected CEMP frequencies agree with the model predictions based on a Salpeter IMF, indicating that the AGB model used in this study is probably not far from reality, at least as applied to low-mass stellar progenitors. However, unlike the case for the giant sample, the top-heavy IMF model does not reproduce the observed trend of the CEMP frequencies for the turnoff stars at all. The combination of these results from the giant and turnoff samples suggests that the current AGB binary-synthesis model may not be suitable for creating carbon-enhanced envelopes for intermediate- to high-mass stars ($3\text{--}8 M_{\odot}$). As the AGB binary-synthesis model (using a Salpeter IMF or a top-heavy IMF) predict far too low frequencies of CEMP stars for our turnoff sample, there likely exists one or more additional mechanisms capable of producing carbon-rich stars below $[\text{Fe}/\text{H}] = -3.0$, the metallicity regime where the CEMP-no stars dominate over the subclass of CEMP-*s* stars.

Funding for SDSS-III has been provided by the Alfred P. Sloan Foundation, the Participating Institutions, the National Science Foundation, and the U.S. Department of Energy Office of Science. The SDSS-III Web site is

<http://www.sdss3.org/>.

SDSS-III is managed by the Astrophysical Research Consortium for the Participating Institutions of the SDSS-III Collaboration including the University of Arizona, the Brazilian Participation Group, Brookhaven National Laboratory, University of Cambridge, Carnegie Mellon University, University of Florida, the French Participation Group, the German Participation Group, Harvard University, the Instituto de Astrofísica de Canarias, the Michigan State/Notre Dame/JINA Participation Group, Johns Hopkins University, Lawrence Berkeley National Laboratory, Max Planck Institute for Astrophysics, Max Planck Institute for Extraterrestrial Physics, New Mexico State University, New York University, Ohio State University, Pennsylvania State University, University of Portsmouth, Princeton University, the Spanish Participation Group, University of Tokyo, University of Utah, Vanderbilt University, University of Virginia, University of Washington, and Yale University.

Y.S.L. is a Tombaugh Fellow. T.S. was supported by the JSPS Grants-in-Aid for Scientific Research (23224004). This work was supported in part by grant PHY 08-22648: Physics Frontiers Center/Joint Institute for Nuclear Astrophysics (JINA), awarded by the U.S. National Science Foundation.

REFERENCES

- Abazajian, K., Adelman-McCarthy, J. K., Agüeros, M. A., et al. 2003, *AJ*, 126, 2081
- Abazajian, K., Adelman-McCarthy, J. K., Agüeros, M. A., et al. 2004, *AJ*, 128, 502
- Abazajian, K., Adelman-McCarthy, J. K., Agüeros, M. A., et al. 2005, *AJ*, 129, 1755
- Abazajian, K., Adelman-McCarthy, J. K., Agüeros, M. A., et al. 2009, *ApJS*, 182, 543
- Abia, C., Busso, M., Gallino, R., et al. 2001, *ApJ*, 559, 1117
- Adelman-McCarthy, J. K., Agüeros, M. A., Allam, S. S., et al. 2006, *ApJS*, 162, 38
- Adelman-McCarthy, J. K., Agüeros, M. A., Allam, S. S., et al. 2007, *ApJS*, 172, 634
- Adelman-McCarthy, J. K., Agüeros, M. A., Allam, S. S., et al. 2008, *ApJS*, 175, 297
- Ahn, C. P., Alexandroff, R., Allende Prieto, C., et al. 2012, *ApJS*, 203, 21
- Aihara, H., Allende Prieto, C., An, D., et al. 2011, *ApJS*, 193, 29
- Allende Prieto, C., Sivarani, T., Beers, T. C., et al. 2008, *AJ*, 136, 2070
- Aoki, W., Beers, T. C., Christlieb, N., et al. 2007, *ApJ*, 655, 492
- Aoki, W., Beers, T. C., Lee, Y. S., et al. 2013, *AJ*, 145, 13
- Aoki, W., Beers, T. C., Sivarani, T., et al. 2008, *ApJ*, 678, 1351
- Aoki, W., Norris, J. E., Ryan, S. G., Beers, T. C., & Ando, H. 2002, *ApJ*, 580, 1149
- Barbuy, B., Spite, M., Spite, F., et al. 2005, *A&A*, 429, 1031
- Beers, T. C., Carollo, D., Ivezić, Ž., et al. 2012, *ApJ*, 746, 34
- Beers, T. C., Chiba, M., Yoshii, Y., et al. 2000, *AJ*, 119, 2866
- Beers, T. C., & Christlieb, N. 2005, *ARA&A*, 43, 531
- Beers, T. C., Preston, G. W., & Shectman, S. A. 1985, *AJ*, 90, 2089
- Beers, T. C., Preston, G. W., & Shectman, S. A. 1992, *AJ*, 103, 1987
- Bisterzo, S., Gallino, R., Straniero, O., Cristallo, S., & Käppeler, F. 2011, *MNRAS*, 418, 284
- Bisterzo, S., Gallino, R., Straniero, O., Cristallo, S., & Käppeler, F. 2012, *MNRAS*, 422, 849
- Bonifacio, P., Spite, M., Cayrel, R., et al. 2009, *A&A*, 501, 519
- Caffau, E., Bonifacio, P., François, P., et al. 2011, *Nature*, 477, 67
- Carollo, D., Beers, T. C., Bovy, J., et al. 2012, *ApJ*, 744, 195
- Chiappini, C. 2013, *AN*, 334, 5951
- Christlieb, N. 2003, *RvMA*, 16, 191
- Christlieb, N., Bessell, M. S., Beers, T. C., et al. 2002, *Nature*, 419, 904
- Christlieb, N., Green, P. J., Wisotzki, L., & Reimers, D. 2001, *A&A*, 375, 66
- Christlieb, N., Schörck, T., Frebel, A., et al. 2008, *A&A*, 484, 721
- Cohen, J. McWilliam, A., Shectman, S., et al. 2006, *AJ*, 132, 137
- Frebel, A., Christlieb, N., Norris, J. E., et al. 2006, *ApJ*, 652, 1585
- Fujimoto, M. Y., Iben, I. Jr., & Hollowell, D. 1990, *ApJ*, 349, 580
- Fujimoto, M. Y., Ikeda, Y., & Iben, I. Jr. 2000, *ApJ*, 529, L25
- Fukugita, M., Ichikawa, T., Gunn, J. E., et al. 1996, *AJ*, 111, 1748
- Gunn, J. E., Carr, M., Rockosi, C., et al. 1998, *AJ*, 116, 3040
- Gunn, J. E., Siegmund, W. A., Mannery, E. J., et al. 2006, *AJ*, 131, 2332
- Hansen, T., Andersen, J., & Nordström, B. 2013, XII International Symposium on Nuclei in the Cosmos, arXiv:1301.7208
- Herwig, F. 2005, *ARA&A*, 43, 435
- Ito, H., Aoki, W., Beers, T. C., et al. 2013, *ApJ*, 773, 33
- Ito, H., Aoki, W., Honda, S., & Beers, T. C. 2009, *ApJ*, 698, L37
- Izzard, R. G., Glebbeek, E., Stancliffe, R. J., & Pols, O. R. 2009, *A&A*, 508, 1359
- Johnson, J. A., Herwig, F., Beers, T. C., & Christlieb, N. 2007, *ApJ*, 658, 1203
- Kobayashi, C., Tominaga, N., & Nomoto, K. 2011, *ApJ*, 730, L14
- Komiya, Y., Suda, T., Minaguchi, H., et al. 2007, *ApJ*, 658, 367
- Korn, A., Grundahl, F., Richard, O., et al. 2007, *ApJ*, 671, 402
- Lau, H. H. B., Stancliffe, R. J., & Tout, C. A. 2009, *MNRAS*, 396, 1046
- Lee, Y. S., Beers, T. C., Allende Prieto, C., et al. 2011, *AJ*, 141, 90
- Lee, Y. S., Beers, T. C., Masseron, T., et al. 2013, *AJ*, in press
- Lee, Y. S., Beers, T. C., Sivarani, T., et al. 2008a, *AJ*, 136, 2022
- Lee, Y. S., Beers, T. C., Sivarani, T., et al. 2008b, *AJ*, 136, 2050
- Lind, K., Korn, A. J., Barklem, P. S., & Grundahl, F. 2008, *A&A*, 490, 777
- Lucatello, S., Beers, T. C., Christlieb, N. C., et al. 2006, *ApJ*, 652, L37
- Lucatello, S., Gratton, R. G., Beers, T. C., & Carretta, E. 2005b, *ApJ*, 625, 833
- Lucatello, S., Tsangarides, S., Beers, T. C., et al. 2005a, *ApJ*, 625, 825
- Luck, R. E., & Bond, H. E. 1991, *ApJS*, 77, 515
- Marsteller, B., Beers, T. C., Rossi, S., et al. 2005, *Nucl. Phys. A.*, 758, 312
- Masseron, T., Johnson, J. A., Plez, B., et al. 2010, *A&A*, 509, 93
- Meynet, G., Ekström, S., & Maeder, A. 2006, *A&A*, 447, 623
- Meynet, G., Hirschi, R., Ekström, S., et al. 2010, *A&A*, 521, 30
- Nomoto, K., Kobayashi, C., & Tominaga, N. 2013, *ARA&A*, 51, 457
- Norris, J. E., Ryan, S. G., & Beers, T. C. 1997, *ApJ*, 488, 350
- Norris, J. E., Christlieb, N., Korn, A. J., et al. 2007, *ApJ*, 670, 774
- Norris, J. E., Yong, D., Bessell, M. S., et al. 2013, *ApJ*, 762, 28
- Pier, J. R., Munn, J. A., Hindsley, R. B., et al. 2003, *AJ*, 125, 1559
- Pols, O. R., Izzard, R. G., Stancliffe, R. J., & Glebbeek, E. 2012, *A&A*, 547, 76
- Richard, O., Michaud, G., & Richer, J. 2002a, *ApJ*, 580, 1100
- Richard, O., Michaud, G., Richer, J., et al. 2002b, *ApJ*, 568, 979
- Roederer, I. U. 2009, *AJ*, 137, 272
- Rossi, S., Beers, T. C., & Sneden, C. 1999, in *The Third Stromlo Symposium, ASP Conference Series*, eds. B.K. Gibson, T.S. Axelrod, and M.E. Putman, 165, p. 264

- Rossi, S., Beers, T. C., Sneden, C., et al. 2005, *AJ*, 130, 2804
Smolinski, J. P., Lee, Y. S., Beers, T. C., et al. 2011, *AJ*, 141, 89
Sneden, C., Cowan, J. J., & Gallino, R. 2008, *ARA&A*, 46, 241
Spite, M., Caffau, E., Bonifacio, P., et al. 2013, *A&A*, 552, 107
Spite, M., Cayrel, R., Hill, V., et al. 2006, *A&A*, 455, 291
Spite, M., Cayrel, R., Plez, B., et al. 2005, *A&A*, 430, 655
Stoughton, C., Lupton, R. H., Bernardi, M., et al. 2002, *AJ*, 123, 485
Suda, T., Aikawa, M., Machida, M. N., & Fujimoto, M. Y. 2004, *ApJ*, 611, 476
Suda, T., & Fujimoto, M. Y. 2010, *MNRAS*, 405, 177
Suda, T., Katsuta, Y., Yamada, S., et al. 2008, *PASJ*, 60, 1159
Suda, T., Komiya, Y., Yamada, S., et al. 2013, *MNRAS*, 432, L46
Suda, T., Yamada, S., Katsuta, Y., et al. 2011, *MNRAS*, 412, 843
Tominaga, N., Iwamoto, N., & Nomoto, K. 2013, *ApJ*, submitted, arXiv:1309.6734
Tominaga, N., Umeda, H., & Nomoto, K. 2007, *ApJ*, 660, 516
Tumlinson, J. 2007, *ApJ*, 664, L63
Umeda, H., & Nomoto, K. 2003, *Nature*, 422, 871
Umeda, H., & Nomoto, K. 2005, *ApJ*, 619, 427
Wisotzki, L., Koehler, T., Groote, D., & Reimers, D. 1996, *A&AS*, 115, 227
Wood P. R., 2011, in Qain S., Leung K., Zhu L., Kwok S., eds, *ASP Conf. Ser. Vol. 451, Proc. 9th Pacific Rim Conference on Stellar Astrophysics* Astron. Soc. Pac., San Francisco, p. 87
Yamada, S., Suda, T., Komiya, Y., Aoki, W., & Fujimoto, M. Y. 2013, *MNRAS*, in press, arXiv:1309.3430
Yanny, B., Newberg, H. J., Johnson, J. A., et al. 2009, *AJ*, 137, 4377
Yong, D., Norris, J. E., Bessell, M. S., et al. 2013, *ApJ*, 762, 27
York, D. G., Adelman, J., Anderson, J. E., Jr., et al. 2000, *AJ*, 120, 1579